[2] Denny, S. B., "Cavitation and Open-Water Performance Tests of a Series of Propellers Designed by Lifting-Surface Method," Rept. 2878, Sept. 1968, Dept. of the Navy, Naval Ship Research and Development Center, Washington, D.C., pp. 39–43.

[3] Timoshenko, S. and Woinowsky-Krieger, S., *Theory of Plates and Shells*, McGraw-Hill, New York, 1959, pp. 33–42.

[4] Boswell, R. J., "Static Stress Measurements on a Highly Skewed Propeller Blade," Rept. 3247, Dec. 1969, Dept. of the Navy, Naval Ship Research and Development Center, Washington, D.C., p. 6-7.

Simplified Tradeoff Studies of Large Hydrofoil Ships

J. R. Greco*
Naval Ship Engineering Center, Hyattsville, Md.

Nomenclature

DHP = drag horsepower, hp
E_H = endurance, hr
L/D = dynamic lift/drag ratio
m_{TO} = takeoff horsepower margin (percent of maximum intermittent horsepower possible)
P_L = payload $\equiv 0.1\ W$, tons
PR = propeller type propulsor system
R = range, naut miles
SHP = maximum intermittent shaft horsepower (engine output), hp
SFC = specific fuel consumption, lb/shp-hr
V = speed, knots
V_{avg} = average speed in sprint/drift mode, knots
V_{burst} = burst speed, short duration capability, knots
V_{max} = maximum continuous operational speed (at maximum continuous shaft hp, which is 85% of SHP), knots
V_{min} = minimum foilborne speed, knots
V_{TO} = takeoff speed from hullborne to foilborne (Fig. 1), knots
W = platform full-load displacement, tons
W_F = fuel capacity, tons
W/S = foil loading, psf
WJ = waterjet type propulsor system
η = propulsive coefficient, Fig. 1; product of transmission (from turbine output shaft) and propulsor system efficiencies
τ_D, τ_S = fractions of time drifting and sprinting, Eqs. (4–6)

Subscripts

D,S = drift and sprint speed modes, respectively

Introduction

THIS Note presents a simple analytical approach for examining first-order effects of major parameters on preliminary designs of large hydrofoil ships. Two design criteria are employed, which reflect the extremes of design speed emphasis: 1) design for a 25% margin (m_{TO}) in horse-power at the takeoff speed V_{TO}, and 2) design for a maximum-burst-speed capability of 50 knots. The powerplants considered are marine gas turbines in three sizes which permit maximum intermittent shaft horsepowers (SHP's) of 30,000, 40,000, and 50,000 hp. (Maximum continuous ratings, which determine maximum cruise speed V_{max}, are 85% of these SHP values.) The two foil loadings considered (W/S = 800 and 1200 psf) are representative of current practical design bounds. The two propulsion types considered (propeller and waterjet) represent the limits (upper and lower respectively) of attainable propulsive efficiency η. This matrix of 2 criteria × 3 SHP's × 2 (W/S)s × 2 propulsor types produces 24 configurations.

Configuration Designs

For each case, the desired design criterion and SHP, W/S, and propulsor type are specified. For the specified W/S and propulsor type, the associated ratio of drag-horsepower to full-load displacement (DHP/W) and η are determined for the design speed of interest (V_{TO} or 50 knots, depending on the design criterion) from Fig. 1. Here DHP/W inversely reflects the L/D capability of the platform, and η is assumed to represent the over-all efficiency of the transmission (from turbine output shaft) and propulsor system. Then W is obtained from the desired design criterion. For the 25% m_{TO} criterion, m_{TO} = 0.25 DHP/W, and

$$W = \frac{\eta \cdot \mathrm{SHP}}{1.25\,(\mathrm{DHP}/W)} \Bigg|_{V_{design} = V_{TO}} \tag{1a}$$

For the 50-knot-burst-speed criterion, $m_{V_{burst}} = 0$, and

$$W = \frac{\eta \cdot \mathrm{SHP}}{\mathrm{DHP}/W} \Bigg|_{V_{design} = V_{burst} = 50\ \mathrm{knots}} \tag{1b}$$

Having determined W, and assuming 0.1 payload fraction (P_L/W = 0.1), the fuel fraction is obtained from the ($P_L + W_F$)/W vs W curve (Fig. 2).

The 24 configurations derived are presented in Table 1. The 50-knot criterion yields lower displacements, except for the 1200/WJ cases. For the 1200-psf foil loading, the difference in the denominators in Eqs. (1a) and (1b) is smaller than the difference in waterjet efficiencies (η) for the two design speeds (V_{TO} = 29 knots; V_{burst} = 50 knots). Similar reasoning associates maximum displacement with the 800/PR designs for the 25% margin criterion and with the 1200/PR designs for the burst-speed criterion.

The maximum burst speeds for the 25% m_{TO} criterion designs were graphically derived by plotting the speed-power curves developed from the powerplant shafthorsepowers and propulsive coefficients (available power) and the platform full load displacements and DHP/W ratio (required power). By plotting these power relationships as a function of speed, the intersection of the available power curve with the required power curve determines the maximum speed (burst) possible, which varies from 39 to 56 knots for the candidate platforms, with little difference between the 800/WJ and 1200/PR designs. The takeoff margins for the burst-speed-criterion designs are well over 25% except for the 1200/WJ designs, which have no margins.

Platform Performance

For each of the 24 configurations, endurance E_H and range R can be calculated for various constant speeds

Received July 6, 1972; presented as Paper 72-595 at the AIAA/SNAME/USN Advanced Marine Vehicles Meeting, Annapolis, Md., July 17–19, 1972; revision received October 10, 1972.

Index category: Surface Vessel Systems.

*Operations Research Analyst.

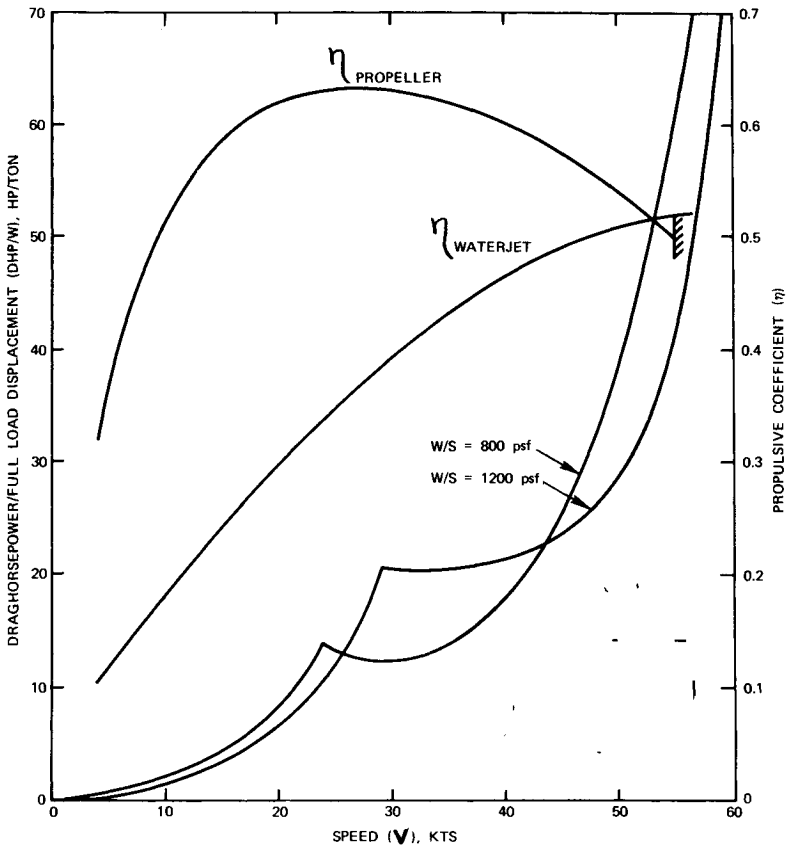

Fig. 1 Primary design parameters.

from $V_{\min}$ to V_{burst}, via the DHP/W and η vs V curves in Fig. 1 and the equations

$$E_H = 2240(0.9\ W_F)\ \eta/[SFC(DHP/W)(W - 0.45\ W_F)] \quad (2)$$

$$R = VE_H \quad (3)$$

In Eq. (2), the term (W − 0.45 W_F) represents the mean displacement, assuming that 0.9 W_F is to be consumed and a 10% fuel reserve (0.1 W_F) is to remain at range R. A constant SFC of 0.60 lb/shp-hr has been assumed for all speeds of operation. The results are presented in Fig. 3a for the 25% m_{T0} criterion and Fig. 3b for the 50-knot-burst-speed criterion. An $E_H - R$ envelope appears for each foil-loading/propulsor combination, with bounds (including SHP levels) as indicated in the legend.

For the 25% m_{T0} criterion, the 800/PR designs are superior in endurance capability over their entire speed regimes because of the high efficiency of the propellers and the low drag horsepower for the 800-psf loading. However, they are speed-limited. The 1200/WJ designs have the lowest endurance, but they are the only designs capable of speeds above 45 knots.

Performance similarities are seen at intersections of the envelopes; e.g., in Fig. 3a, the 1200/PR and the 800/WJ designs both achieve 45-hr endurance and 1650-naut-mile range at a speed of 36.5 knots.

The endurance for various configurations can be related to the full-load displacements in Table 1. For example, for the 800/PR design, E_H is increased by 5% (78 hr to 82 hr) when SHP and W are increased by 67% each (30,000 to 50,000 shp, and 1103 to 1838 tons). Likewise for the 40,000-shp/propeller configuration, a 49% increase in displacement (985–1471 tons), going from a 1200 psf foil loading to 800 psf, yields a 74% increase in E_H (46 hr vs 80

Table 1 Configurations computed

			(m_{TO} = 25%; $V_{\text{design}} = V_{TO}$)							($V_{\text{design}} = V_{\text{burst}}$ = 50 knots)				
	W/S, psf	SHP, hp	V_{TO} knots	$V_{\min}$, knots	W, tons	P_L, tons	W_F/W	$V_{\max}$, knots	V_{burst}, knots	W, tons	P_L, tons	W_F/W	m_{TO}, %	$V_{\max}$, knots
1	800-PR-30000		24	28	1103	110	0.374	36	39	395	40	0.312	249	49
2	800-WJ-30000		24	28	590	59	0.344	43	45	376	38	0.306	96	48
3	1200-PR-30000		29	32	739	74	0.357	39	45	600	60	0.345	53	46
4	1200-WJ-30000		29	32	457	46	0.320	52	56	564	56	0.341	0	40
5	800-PR-40000		24	28	1471	147	0.380	36	39	527	53	0.334	248	49
6	800-WJ-40000		24	28	787	79	0.360	42	45	496	50	0.331	98	48
7	1200-PR-40000		29	32	985	99	0.370	38	46	800	80	0.363	53	46
8	1200-WJ-40000		29	32	602	60	0.346	52	56	753	75	0.360	0	40
9	800-PR-50000		24	28	1838	184	0.385	36	39	659	66	0.350	248	49
10	800-WJ-50000		24	28	983	98	0.370	42	45	620	62	0.347	98	48
11	1200-PR-50000		29	32	1231	123	0.377	39	46	1000	100	0.372	53	46
12	1200-WJ-50000		29	32	753	75	0.359	52	56	941	94	0.370	0	40

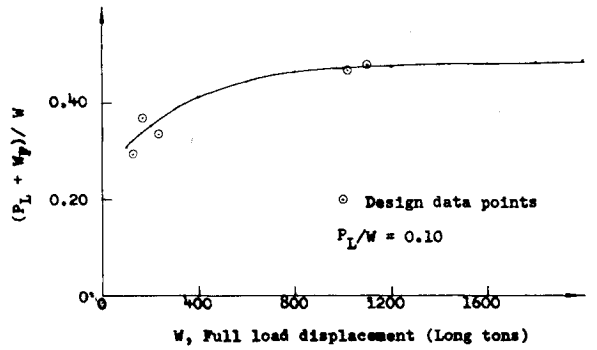

Fig. 2 Load fraction vs full load displacement.

hr). Thus, the reduction in foil-loading yields a greater endurance gain per ton added ($\Delta E_H/\Delta W$ = 0.070 hr/ton) than does the SHP increase (0.006 hr/ton). A change from waterjet to propeller propulsion for the 30,000-shp/800-psf cases yields $\Delta E_H/\Delta W$ = 0.66 hr/ton.

Figure 3b (burst-speed criterion) indicates generally the same trends as Fig. 3a. The major differences result from the facts that a) a decrease in foil loading reduces displacement (see Table 1), contrary to the trend for the 25% m_{TO} criterion, and b) at 50 knots the difference in η between propeller and waterjet is minimal.

For 800/*PR* designs, 67% increases in SHP and W yield a 15% increase in E_H (62.5–72 hr). As a result, $\Delta E_{H_{\max}}/\Delta W$ = 0.036 hr/ton. A foil loading increase (800–1200 psf) for 40,000 shp/propeller designs results in a 35% decrease in E_H (68–44 hr) while displacement increases by 52% (527–800 tons), so that $\Delta E_H/\Delta W$ = −0.088 hr/ton. A change from water jet to propeller propulsion for the 30,000 shp/800 psf design yields $\Delta E_H/\Delta W$ = 1.26 hr/ton.

The sensitivity of the results to the DHP/W characteristics employed can be seen by considering 40,000-SHP cases and the 25%-m_{TO} criterion. For the 800/*PR*, 800/*WJ*, 1200/*PR*, and 1200/*WJ* designs, Table 1 shows displacements of 1471, 787, 985, and 602 tons, respectively. The associated endurances at 35 knots are 69.3, 45.4, 44.6,

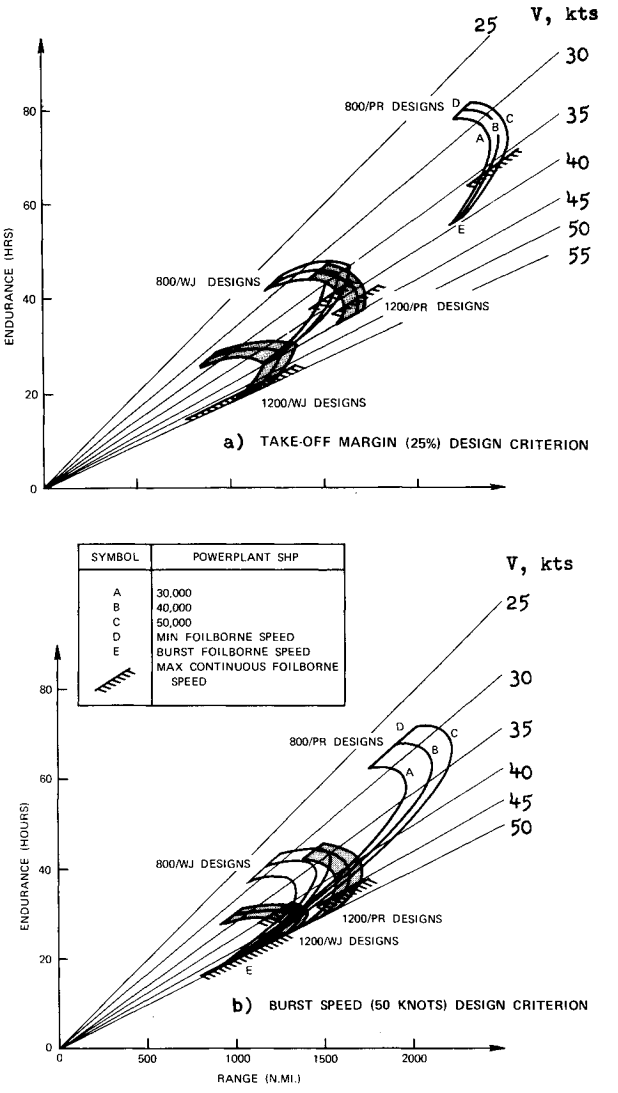

Fig. 3 Endurance range maps.

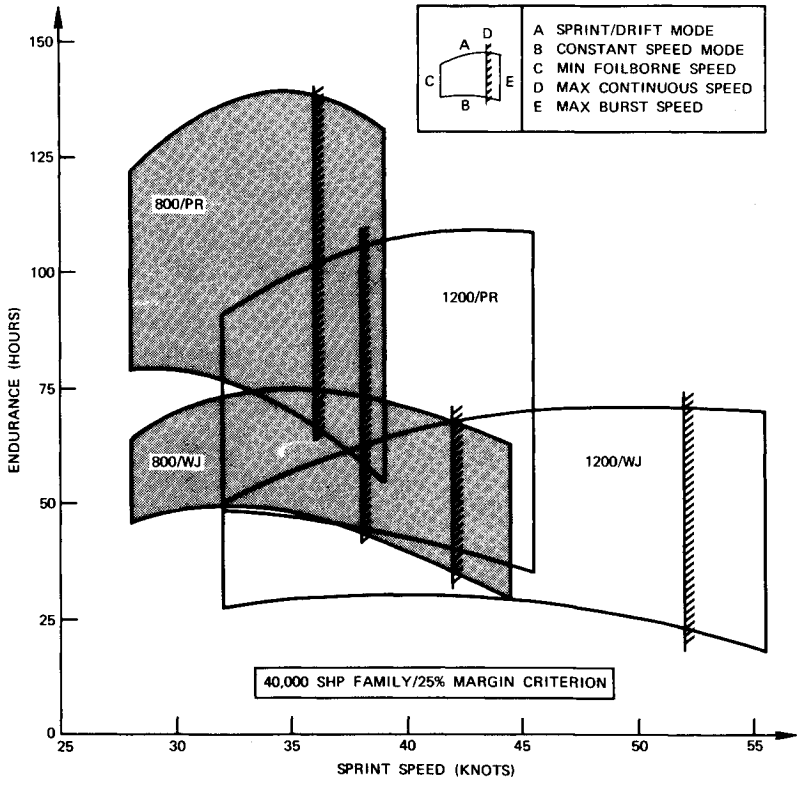

Fig. 4 Performance comparison (sprint/drift mode vs constant speed).

and 28.9 hr, respectively (Fig. 3a). If the drag horsepower were increased by 3000 hp, causing increases in (DHP/W) of 17, 38, 17, and 32% for the four designs, their endurances would be reduced by 15, 32, 16, and 29%, respectively.

Sprint/Drift Performance Mode

The performance capability of the 40,000-SHP family (25% m_{T0} criterion) was also calculated for a mode of operation in which the hydrofoil would alternately sprint at speed V_S and then drift at speed V_D (hullborne, with its engine virtually idling). Let the fraction of time sprinting be τ_S, and the fraction of time drifting be τ_D ($\tau_S + \tau_D = 1$). The sprint/drift time split depends upon the assumed average speed for the cycle V_{avg} (assumed to be 20 knots), the sprint speed V_S (variable), and the drift speed V_D (assumed to be 10 knots). Equations (2) and (3) become:

$$E_H = \frac{2240\ (0.9\ W_F)}{(\mathrm{SFC})(W - 0.45\ W_F)[(\tau_S/\eta_S)(\mathrm{DHP}/W)_S + (\tau_D/\eta_D)(\mathrm{DHP}/W)_D]} \quad (4)$$

$$R = E_H(\tau_S V_S + \tau_D V_D) \qquad (\tau_S + \tau_D = 1) \quad (5)$$

where

$$\tau_D = (V_S - V_{avg})/(V_S - V_D) = (V_S - 20)/(V_S - 10) \quad (6)$$

Figure 4 compares results from Eq. (4) with the constant-speed results from Eq. (2). Endurances are significantly increased by sprint/drift operation, and maximum endurance is attainable at a higher (sprint) speed than in the constant-speed case (e.g., 34 vs 29 knots for 800/PR).

Concluding Remarks

The relationships among first-order hydrofoil design parameters and design criteria have been examined in a cursory manner for large hydrofoil configurations. The results in Table 1 and Fig. 3 can be used to select first-order designs for various characteristics. For example, for maximum endurance with a 25% margin on thrust at takeoff speed (Fig. 3a), a configuration with 800-psf foil loading and propeller propulsion would be chosen, but it would be limited in maximum speed to 36 knots (Table 1), which is low compared to other configurations. A cursory look at the sprint/drift mode of operation has indicated that it can significantly improve endurance capability.

The analysis should be expanded to address effects of additional parameters of interest and employ refined design and performance equations. The sensitivities of the speed, endurance, and range results to operational speed mode, incremental drag horsepower, payload fraction, and SFC variations with powerplant size and vehicle speed, should be explored.

References

[1]Clarke, H. D., "Draft Hydrofoil Design Technical Note," TN 6112-71-4, May 1971, Naval Ship Engineering Center, Hyattsville, Md.

[2]Greco, J. R., "Large Hydrofoil Ships Feasibility Level Characteristics (U)," TN 6112-72-5, Jan. 1972, Naval Ship Engineering Center, Hyattsville, Md.

[3]Mandel, P., *Water, Air, and Interface Vehicles*, MIT Press, Cambridge, Mass., 1969.

[4]Sejd, J. J., "Hydrofoil Endurance, Speed, and Mission," June 1971, Naval Ship Engineering Center, Hyattsville, Md.

Analysis of Gas Bubble-Liquid Coflow Systems

Robert L. Stoy* and Peter P. Ostrowski†
University of Connecticut, Storrs, Conn.

Nomenclature

A = flow cross section area
D = bubble diameter
E = entrainment rate
F_s = shear force on nozzle walls
f = viscous correction
g = acceleration of gravity
h_s = bubble surface heat-transfer coefficient
k = added mass coefficient
$\dot{m}$ = mass flow rate
Nu = Nusselt number
Pr = Prandtl number
$\dot{q}$ = heat flux
R = gas constant
T = static temperature
V_B = bubble volume
α = bubble volume fraction
κ = thermal conductivity
σ = surface tension coefficient
$(\ )_B$ = bubble
$(\ )_L$ = liquid

Introduction

DURING the course of an investigation of trajectories of thermal effluents, the aeration of the jet water to enhance turbulent mixing was proposed. The present one-dimensional analysis was undertaken to provide a better understanding of the effects of air bubbles on thermal jets, and to provide a foundation for developing an experimental study of thermal jets with aeration. Furthermore, there is presently no general one-dimensional analysis of a bubble-liquid coflow available in the literature, a situation that seems surprising considering the uses to which these flows are put. In a recent study by Cederwall and Ditmars[1] a related problem of destratification of a lake by an air-bubble plume was considered. They used a two-dimensional analysis in which the bubble plume is assumed to act like a jet, with a simple jetlike entrainment model, that produced successful results. Other work on a water-air bubble coflow system has been carried out by Muir and Eichhorn[2] in a study of air-augmented water propulsion systems. They investigated nozzle flows with the intent of increasing thrust levels by making use of the slip velocity of the bubbles. That is, augmented thrust can be obtained since the bubbles move faster than the water in an accelerated flow. Another area in which air-water coflow is used is that of activated sludge aeration in which air-bubble plumes are employed to promote mixing and to provide oxygen for the micro-organisms which break down the organic materials.

Analysis

A simple one-dimensional analysis is considered to be appropriate for this study of aerated water jets. The following assumptions are made: steady flow, no coalescence or breakup of bubbles, no viscous dissipation effects, a thermally and calorically perfect gas, and no interaction

Received May 12, 1972. The authors acknowledge the assistance of the University of Connecticut Computer Center supported by National Science Foundation Grant GJ-9.

Index categories: Propulsion System Hydrodynamics; Hydrodynamics.

* Associate Professor of Mechanical and Aerospace Engineering. Member AIAA.

† Graduate Student. Associate Member AIAA.